ChemCommun

Supplementary Information

High-porosity carbon molybdenum sulphide composite with enhanced electrochemical hydrogen evolution and stability

Anders B. Laursen, Peter C. K. Vesborg, and Ib Chorkendorff*

Experimental section:

MoS_x HER catalysts were prepared according to the procedure published by our group and X. Hu's group (1,2). In short, 2 mM $(NH_4)_2MoS_4$ in 0.1 M $NaClO_4$ aqueous solutions were prepared in an Ar glovebox. The solution was sealed and sonicated for ca 10 min before transferring into the H-cell under continued Ar flow. The solution was then bubbled with Ar for 20 min before experiments were started to remove any oxygen from the solution. Depositions were all done by cycling the working electrode potential between -0.366V to 0.734V vs RHE (pH 7.4), the number of cycles determined the amount of catalyst deposited. In the work X. Hu's group (2) it was determined that the maximal activity was achieved after 18 cycles and that film thicknesses did not increase beyond approx. 35 cycles. We have previously determined comparable activities to the best of the X. Hu groups after 19 CV cycles (1). Thus the base line for our present comparison was the 19 CV deposition. All aqueous solutions are prepared with water from a MilliPore water system (18.2 MΩ). All glassware are cleaned in Piranha (1:3 30% H_2O_2 in conc. H_2SO_4) and sonicated in water 3 times before use.

Electrochemical measurements:

A custom made H-cell is used for all the measurements (3). The reference electrode is a commercial Hg/Hg_2SO_4 (saturated K_2SO_4) with a potential of 680 mV vs. NHE. All potentials in this work are corrected by $E_{corr.} = E_{measured} + 0.680\ V + pH \cdot 0.059\ V$. The reference electrode Luggin is separated from the working electrode compartment by a glass-fritt during MoS_x deposition the Luggin is filled with saturated NaCl and during HER activity experiments with 1M $HClO_4$. The purpose of the NaCl salt-bridge is to protect the reference electrode from the $(NH_4)_2MoS_4$ solution. IR correction were determined using the Biologic potentiostat EIS single point ohmic drop measurement for several electrodes and the average value (15 Ω) was used to correct the obtained data. Data were corrected using the equation: $E_{corrected}(V) = E_{measured}(V) - 15\Omega \cdot I_{measured}(A)$.

Electrode preparation:

C-paper electrodes: Electrodes were made by cutting carbon paper (untreated carbon paper, Carbon paper – 2050-A, from FuelCellStore.com) into 10 cm wide strips. These strips were then placed on a 110°C hotplate and a thin line of water dispersed Teflon (Dyneon TF5032R PTFE) was put approximately 1 cm from the long end of the strip. When dried, a thin white line showed the Teflon barrier. This barrier had the purpose of stopping any electrolyte from diffusing into the porous network and up to the contact point, which could cause a parasitic corrosion current. The strip of carbon paper was then cut into electrodes 0.5 cm wide. A piece of copper wire was then curled into a spiral in one end. The spiral was placed on the contact point of the electrode (1 cm above the Teflon line) and covered in silver paste (HighPurity Ag paint SPK supplies). After drying on a hotplate at 110°C the wire was slipped into a Pyrex tube. Next, the end of the glass tube and the top of the electrode — all the way onto the Teflon barrier — was covered in a hot-melt glue (from a local hardware supplier, Bosch). After hardening, the electrode was masked off to expose 0.5 x 0.5 cm by wrapping the electrode in self-adhesive Teflon tape (Saint Gobain). The mask allowed only 1 cm^2 to be exposed to the electrolyte. After deposition of the catalyst a clear dividing line showed where the electrode had been exposed to the electrolyte. This well-defined line showed that the mask worked according to the intention. It is acknowledged that the geometric area was not equivalent to the actual electrode surface but taking the effect of electrode porosity into account, the effect of any electrolyte diffusing up under the mask was deemed negligible.

Act-C-Paper: The C-paper electrodes were activated immediately before use by immersing just the un-masked area of the prepared electrodes into a freshly prepared solution of piranha (1:3 vol. equivalents 35% H_2O_2(aq) /conc. H_2SO_4). The electrodes were left to react 30-60 sec then rinsed by immersion in clean Millipore water three times each time soaking ~1 min. If the mask was removed after activation the solution was seen not to wet the carbon higher than the mask.

FTO electrodes: FTO 1 1/4" x 2" pieces were washed by ultra sonication sequentially in acetone, isopropanol, and three times Millipore water. After drying a piece of copper wire was twisted into a coil in one end and fixed to one end of the conductive side of electrode using silver paste. After drying a glass tube was slipped over the copper wire down to the contact point, the tube end and contact were then covered in hot-melt glue. When cured the active area (1-3cm^2) was masked off using self-adhesive Teflon tape. Just prior to use the surface was cleaned with a drop of piranha solution and rinsed thoroughly in Millipore water.

Catalyst deposition on porous carbon fibre electrodes:

The MoS_x catalyst was deposited according to the procedure described above. Fig. S1 shows the CVs of the electrochemical deposition. The four features at -0.35 V vs RHE, -0.15 V vs RHE, 0.35 V vs RHE, and 0.7 V vs RHE are attributed to the catalyst deposition. The feature at 0.7 V vs RHE and -0.35 V vs RHE are identified to be MoS_3 and MoS_2 deposition, respectively (2). The other two features are not understood at present.

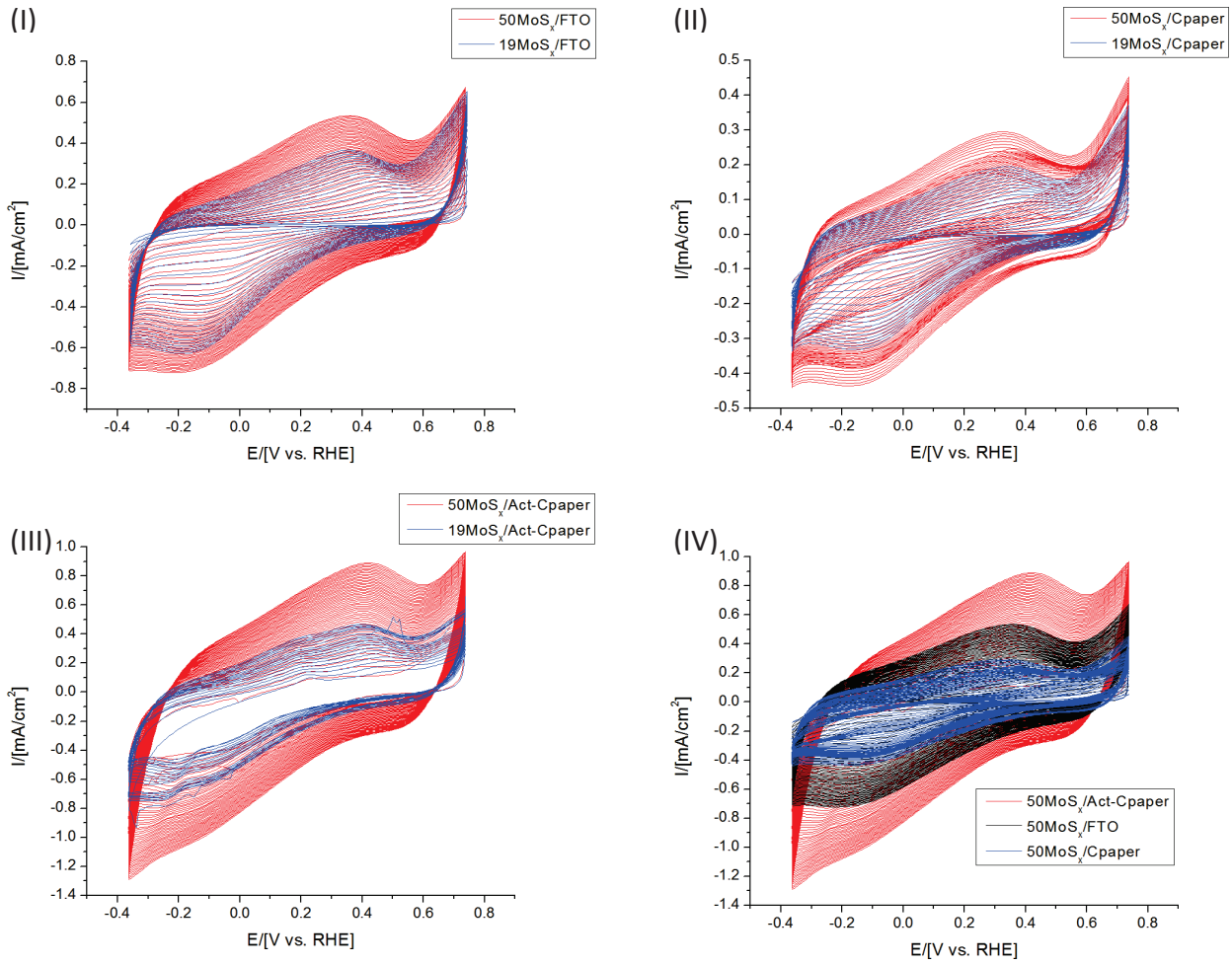

Fig. S1 Deposition CVs on (I) FTO, (II) C-paper, and (III) Act-C-paper for 19 (blue) and 50 (red) CV cycles, respectively. (IV) comparison of 50 CV cycles for Act-C-paper (red), FTO (black), and C-paper (blue). See above for deposition solution composition.

From Fig. S1 it was determined that the Act-C-paper electrodes had more MoS_x deposited than the flat FTO electrodes in a similar amount of cycles. It was inferred that the deposition throughout the porous electrode would be more mass-transport limited than on a flat electrode, hence it was attempted to increase the number of deposition cycles beyond the 35 that was know from literature to be the maximal number increasing catalyst deposition on FTO (2).

Table S1 Table of electrode properties:

Catalyst	Tafel slope	$J_0^{exchange}$ / [A/cm^2]	C_{dl}/ [mF/cm$^2_{geo}$]	Surface roughness ratio	Approximated surface area /[cm^2/cm$^2_{geo}$]
MoS_x(19CV)/FTO	93.1	1.68E-05			
MoS_x(50CV)/FTO	66.8	7.99E-06			
MoS_x(19CV)/C-paper	38.9	2.97E-08			
MoS_x(50CV)/C-paper	36.6	5.07E-08			
MoS_x(19CV)/Act-C-paper	44.3	1.40E-06			
MoS_x(50CV)/Act-C-paper	38.4	1.06E-06			
C-paper			1.31E-2	1	5.23E-1
Act-C-paper			0.62E-1	4.8	2.49

Electrochemical surface area determination:

The electrochemical surface area was determined by CV cycling a C-paper and Act-C-paper electrode in the potential region 0.10–0.20 V vs RHE at scan speeds from 5–200 mV/s. This potential region was chosen because no other feature than the capacitance was observed here. Plotting the current difference from the forward and reverse scan at 0.15 V vs RHE as a function of scan speed a linear response was obtained. At the lowest scan speed (5mV/s) the linear behaviour was not observed and thus the point excluded in the following procedure. The total double layer capacitance (C_{dl}) is twice the slope of the linear response of ΔI/scan speed (2,4): from this $C_{dl,C\text{-}paper}$ = and $C_{dl,Act\text{-}C\text{-}paper}$ = could be isolated. This quantity is material dependent and therefore only the relative response between the two electrodes could be determined accurately. However, as the area averaged capacitance of carbon materials may be approximated as 25 μF/cm^2 (4) the approximate surface area was calculated as well as the relative electrochemical surface area increase upon the acid treatment. The results are shown in Tabl. S1.

Figure showing the electrochemical response to changed scan speed for C-paper and Act-C-paper electrodes.

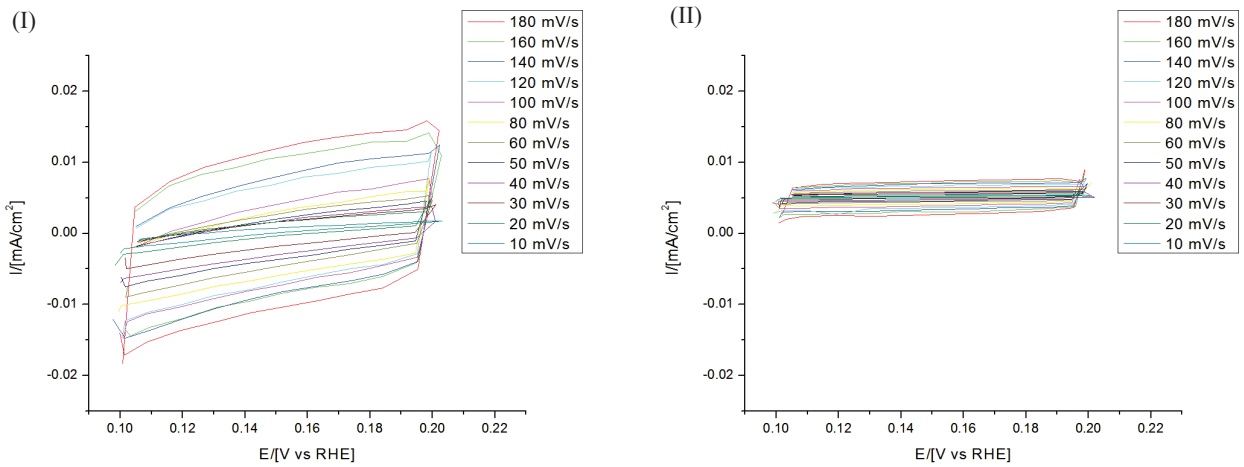

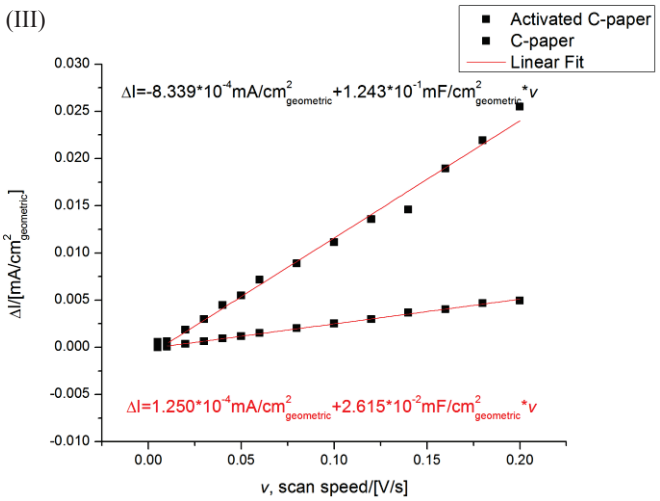

Fig. S2 CV in capacitive region for (I) Act-C-paper and (II) C-paper with varying scan speeds between 5 and 200 mV/s. (III) linear correlation of capacitance currents measured at 0.15 V vs. RHE. Showing results of least square linear regression at scan rates above 5 mV/s.

Table S2 Table summarizing the results of the surface area analysis for the C-paper and Act-C-paper electrodes without catalyst deposition. Approximated surface area is calculated based on an average surface capacitance of 25 μF/cm^2 (4) for carbon.

Electrode	C_{dl}/[mF/cm$^2_{geo}$]	Surface roughness ratio	Approximated surface area /[cm^2/cm$^2_{geo}$]
Act-C-paper	0.62E-01	4.8	2.49E+00
C-paper	1.31E-02	1.0	5.23E-01

Tafel analysis:

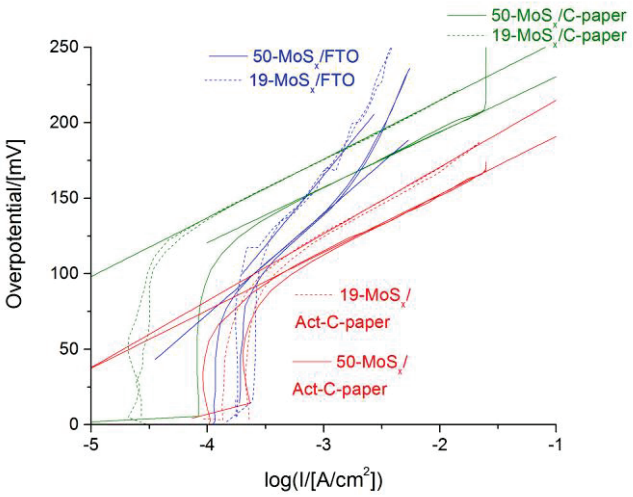

Fig. S3 CV at 5mV/sec for Tafel analysis of the MoSx(19CV)/FTO, MoSx(50CV)/FTO, MoSx(19CV)/C-paper, MoS_x(50CV)/C-paper, MoS_x(19CV)/Act-C-paper, MoS_x(50CV)/Act-C-paper. 1M HClO4, using a Hg/HgSO4 as the reference electrode and H_2 bubbled Pt mesh as the counter electrode.

Tafel analysis performed on the MoSx deposited electrodes. Due to the noise caused by bubbling on the FTO electrodes the data had to be further smoothed before an accurate Tafel analysis could be performed. It should be noted that the FTO electrodes show a lower Tafel slope than what others and we have reported previously (1,2,5,6). This was attributed to these electrodes showing an unusual early mass transport limited current, seen by the curve showing two linear regions at low overpotentials.

ChemCommun

Supplementary Information

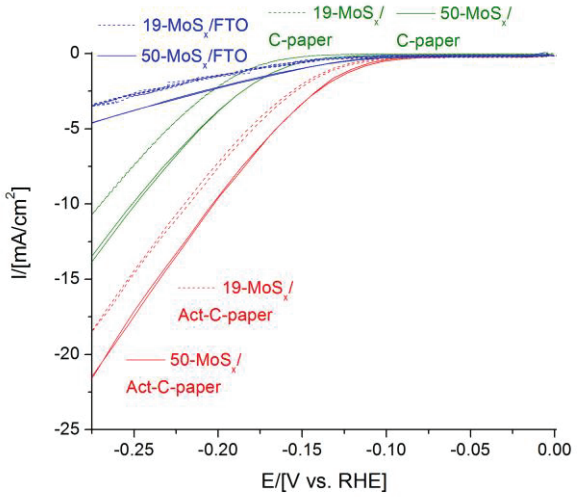

Fig. S4 non-IR compensated CV of the MoSx(19CV)/FTO, MoSx(50CV)/FTO, MoSx(19CV)/C-paper, MoS_x(50CV)/C-paper, MoS_x(19CV)/Act-C-paper, MoS_x(50CV)/Act-C-paper. 1M $HClO_4$, using a $Hg/HgSO_4$ as the reference electrode and H_2 bubbled Pt mesh as the counter electrode.

References

1 B. Seger, A. B. Laursen, P. C. K. Vesborg, T. Pedersen, O. Hansen, S. Dahl and I. Chorkendorff, *Angew. Chem. Int. ED.*, 2012, **51**, 9128.
2 D. Merki, S. Fierro, H. Vrubel and X. Hu, *Chem. Sci.*, 2011, **2**, 1262.
3 A. B. Laursen, S. Kegnæs, S. Dahl and I. Chorkendorff, *Energ. Environ. Sci.*, 2012, **5**, 5577.
4 B.E. Conway, V. Birss, J. Wojtowicz, *J. Power Sources*, 1997, **66**, 1.
5 D.Merki, H. Vrubel, L. Rovelli, S. Fierro and X. Hu, *Chem. Sci.*, 2012, **3**, 2515.
6 H. Vrubel, D. Merki, X. Hu, *Energ. Environ. Sci.*, 2012, **5**, 6136.